EFFECTS OF FROZEN ROCK ON EXPLOSIVE COUPLING

Mark Leidig[1], Jessie Bonner[1], Randy Martin[2], Sara Dougherty[1] and Katherine Murphy[1]

Weston Geophysical Corp.[1], New England Research, Inc.[2]

Sponsored by Air Force Research Laboratory

Contract No. FA8718-04-C-0026

ABSTRACT

Laboratory studies have demonstrated that frozen rock is significantly stronger than unfrozen rock, and it has been hypothesized that this increased strength can significantly alter seismically estimated yield. Weston Geophysical Corporation conducted the Frozen Rock Experiment (FRE) in central Alaska in August 2006 to provide empirical data in order to test the hypothesis. This region of Alaska has abrupt lateral boundaries in discontinuous permafrost, and we detonated 3 shots in frozen rock and 3 shots nearby in unfrozen rock ranging in size from 200 to 350 lbs. Nearly 125 accelerometers and seismometers were deployed specifically for this experiment at distances of 10 m to over 20 km. Videographic and velocity of detonation data were also collected. The data from this experiment are being analyzed to aid in determining actual yield for explosions in permafrost regions.

We developed a 1-D velocity model for the test site region using refraction analyses and inversion of surface wave dispersion and receiver functions. During development of this model, we found evidence of seismic anisotropy in the shallow crust. This model, with inclusion of the anisotropy, fit the observed *P*- and *S*-wave arrivals well, but predicted a later arrival for the surface waves than was observed. Therefore, we initiated development of a 3-D velocity model for the region that could account for lateral velocity changes. Laboratory analysis of test site rock samples document the rheologic differences of the test site medium when both frozen and unfrozen. Velocities increased ~12% for V_p and V_s when the sample was frozen to below -10 °C. Elastic moduli also showed significant increases in the frozen samples. These results are in agreement with prior studies and are indicative of the increased strength of frozen rock.

The explosive source is being defined in various ways. Theoretical Mueller-Murphy (MM) source spectra were generated using the test site seismic velocities determined *in-situ*. Ratios of the unfrozen/frozen spectra were computed. Although there are no calibrated MM rock properties for gneiss or schist, which are found in the test site, modeling indicates that MM spectra generated from a rhyolite model fits the observed data well when the differences in the test site velocities are considered. In addition, recordings on close-in accelerometers and seismometers provide data for moment tensor inversions, which help define the symmetry and phenomenology of the explosions. Dr. Charlie Sammis has performed extensive analysis modeling the damage around an explosive source. His model involves multiple zones of rock pulverization and fracturing. It is hypothesized that displacement along small fractures, integrated over the entire damage volume, can produce the large shear waves observed from explosions. The model is dependant on the rock strength, which has been shown to increase in frozen rock. We are collaborating to provide him with data to validate his model.

Spectral analyses were conducted to determine the differences in seismic phases generated by the explosions. Spectral ratios of the full waveform for equal yield detonations show that frozen shots produced larger vertical spectral amplitudes at all frequencies, except between approximately 4 and 9 Hz. In this frequency range, the unfrozen shots were up to 1.4 times larger, while above 10 Hz, the frozen shots were 4 times larger.

Large shear waves are observed in the FRE data. Broadband transverse components, as close as 3 km, show a large amplitude arrival just prior to the Rayleigh wave, which could be a Love or SH wave. Record sections of the Texan recordings clearly show an arrival we determined to be a shear wave. The *P*/*S* ratio appears to vary depending on the shot type and may therefore provide important information on the mechanics of shear wave generation from an explosive source.

OBJECTIVES

Weston Geophysical Corporation conducted the Frozen Rock Experiments (FRE) in central Alaska to characterize the variations in ground motion scaling and coupling for explosions in frozen and unfrozen rock. We recorded the explosions on a large array of near-source and local stations deployed specifically for the experiment. The data are currently being analyzed to quantify the variations observed. The results will be interpreted to help understand possible biases in the estimation of seismic yield from explosions in frozen rock.

RESEARCH ACCOMPLISHED

Experiment Background

A critically important aspect of nuclear test monitoring is yield estimation. United States monitoring agencies must be able to accurately estimate yields for nuclear explosions detonated in regions of monitoring concern. If frozen-rock emplacement conditions create a circumstance favorable for biased yields, data must be available such that any bias can be accounted for when the yield is estimated. Prior studies (Mellor, 1971) have established that frozen-rock properties are considerably different from unfrozen-rock properties. Moreover, it has been hypothesized that these altered properties may be sufficient to cause significant variations in seismic coupling, which in turn, significantly alters seismic yield estimates.

Sammis and Biegel (2004) noted that an increase in low-temperature uniaxial strength is related to the ice in the initial pores and cracks. The ice increases the apparent coefficient of sliding friction on these initial cracks. Since the strengthening is strain-rate dependent, for nuclear explosions the full strengthening should occur in a small range near 0 °C. Increasing the seismic velocity and/or rock strength would cause reduced seismic amplitudes in the far-field for explosions in frozen rock, which would result in an underestimated yield.

Experiment Location and Design

We conducted the experiment just north of Fairbanks, AK because that region contains discontinuous permafrost, with frozen and unfrozen rock in close proximity. Farther north, it is difficult to find unfrozen rock and farther south, it is difficult to find frozen rock. Figure 1 shows the location of the FRE test sites and locations of some of the seismic sensors deployed specifically for this project. The diagram in Figure 2 shows a cross-section of the FRE test site. Explosions of 200 and 350 lb of ammonium nitrate fuel oil (ANFO) were conducted in a gneiss/schist at the frozen test site in Goldstream Valley. A third frozen rock explosion of 350 lb was conducted in frozen gravels. The hill overlooking the valley is composed of unfrozen, dry schist and is where we detonated three shots of 100, 200, and 350 lb. In general, the centroid depth of the shots was between 6 and 8 m. All tests detonated as planned with the exception of shot 5 (350 lbs unfrozen), which cratered.

High-g accelerometers and short-period seismometers were deployed at near-source distances to record the shot time and source phenomenology of the explosions. The data are being analyzed to ascertain spall effects and compute moment tensors. Broadband and vertical component (“Texan”) seismometers were deployed at local distances to help quantify phase generation and propagation. High-resolution videographic data were recorded to verify the explosions detonated as planned and to analyze surface phenomenology.

Laboratory Analysis

Rock samples from the test sites were sent to New England Research, Inc. for analysis. The physical rock properties of each sample were measured both saturated and dry at room temperature, and then the measurements were performed again when the samples were chilled to below -10 °C. Seismic velocities and elastic moduli are shown in Figure 3. Both the compressional and shear velocities increased ~12% when frozen. In addition to the velocity increases, the bulk modulus, Poisson’s ratio, and uniaxial strain increased 36%, 26%, and 28%, respectively when the samples were frozen. These findings are in agreement with previous studies of frozen rock properties and indicate a much stronger rock at the frozen test site than the unfrozen site.

The increased strength is caused by freezing the water in a rock’s pores and cracks and was observed in the field with velocity of detonation recorders (VODRs), which showed an increase in explosive performance for the frozen shots. A stronger rock better confines the explosion and causes a faster explosive burn rate. This also results in a smaller explosive cavity radius and reduced sliding along pre-existing fractures.

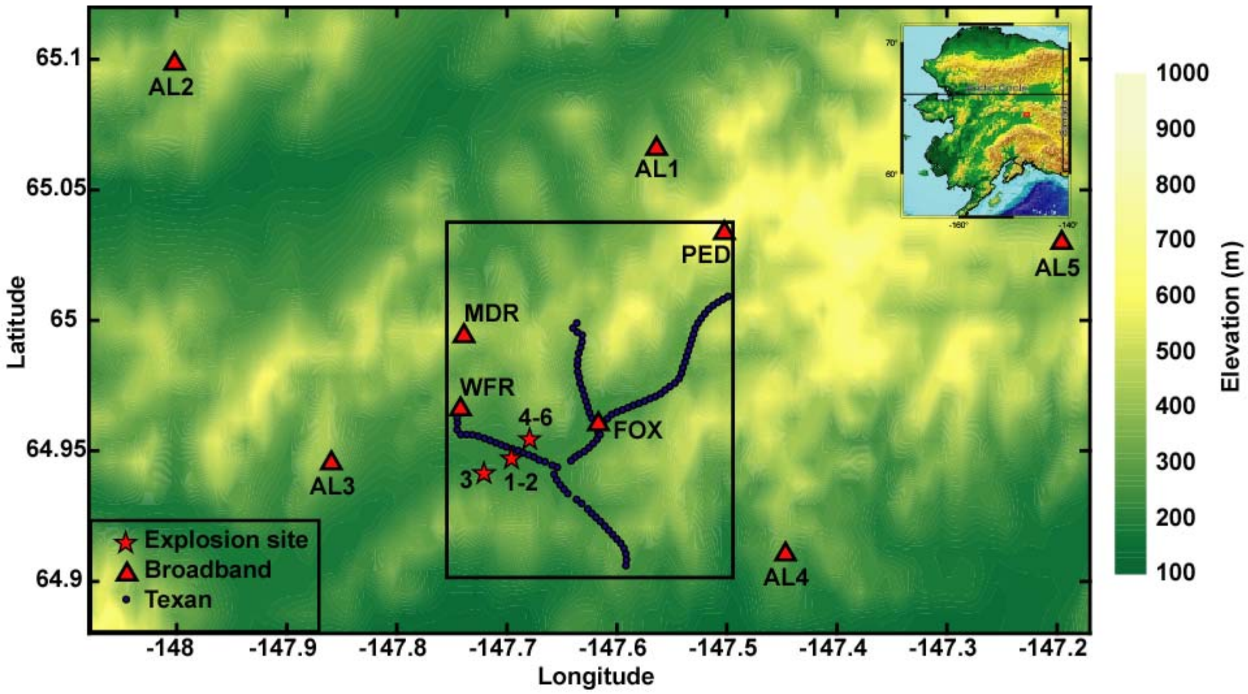

Figure 1. Location map of the test site region. Shot locations (stars) and deployed seismic stations (triangles and dots) are shown. Close-in accelerometers and seismometers are not shown.

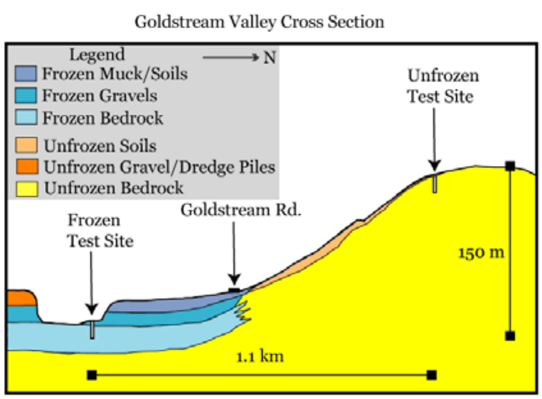

Figure 2. Cross-section of the test site. The frozen shots were located in a valley and the unfrozen shots were detonated on a hill overlooking the valley.

Velocity Model

To determine the in-situ velocity model for the test site, we combined shallow test site refraction data with Texan recordings of the shots and teleseismic earthquake receiver functions to develop a 1-D velocity model. The shallow refraction profiles were collected prior to detonation of the shots with a hammer source and a 60-channel recorder. An analyst picked the first breaks, which were combined with standard refraction equations to determine the *P*-wave velocity, while the ground roll was inverted to calculate the shear wave velocity. We then used the Texan shot recordings to perform similar analyses at deeper depths. It was observed on the Texans that the *P*-wave arrival times were azimuth dependent (Figure 4). A velocity anisotropy of ±10% and a fast direction of ~70° best removed the azimuthal dependence. The corrected Texan travel times can be observed on the right side of Figure 4.

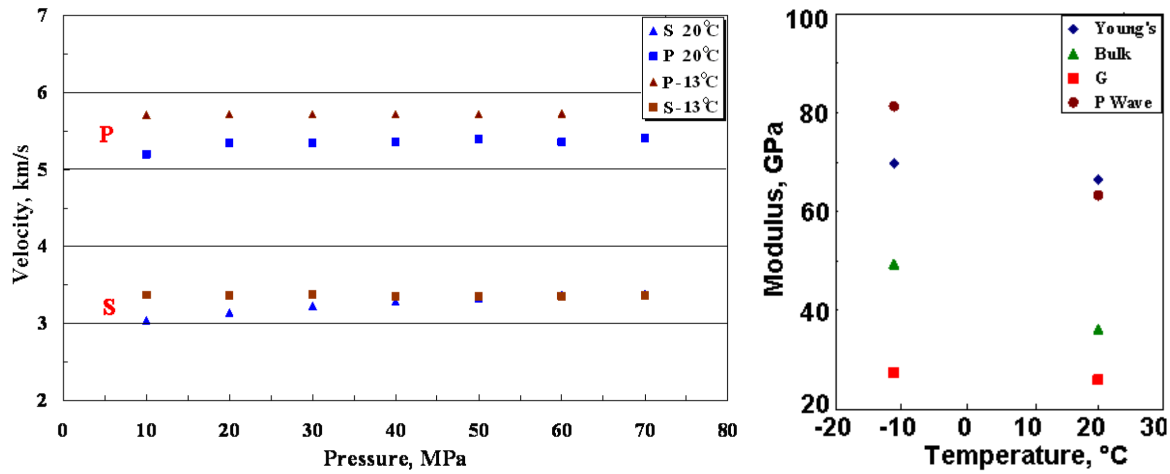

Figure 3. Ultrasonic *P*- and *S*-wave velocities (left) and elastic moduli (right) for a test site rock sample at room temperature and frozen.

To determine the velocity in the remainder of the crust, receiver functions from teleseismic earthquakes were jointly inverted with surface wave dispersion from the FRE shots recorded on nearby broadband seismometers (Figure 5). A niching genetic algorithm (Koper et al., 1999) was used to search the parameter space for the best fitting model. Figure 6 plots this (red) and the range of models that adequately fit the observed data.

This 1-D model fit the observed *P* and *S* arrivals very well, but the surface waves arrived earlier than predicted by the model at some stations. We are developing a 3-D model to better fit the surface wave arrivals. The final velocity model will be used in moment tensor inversions to examine the source phenomenology of the explosions.

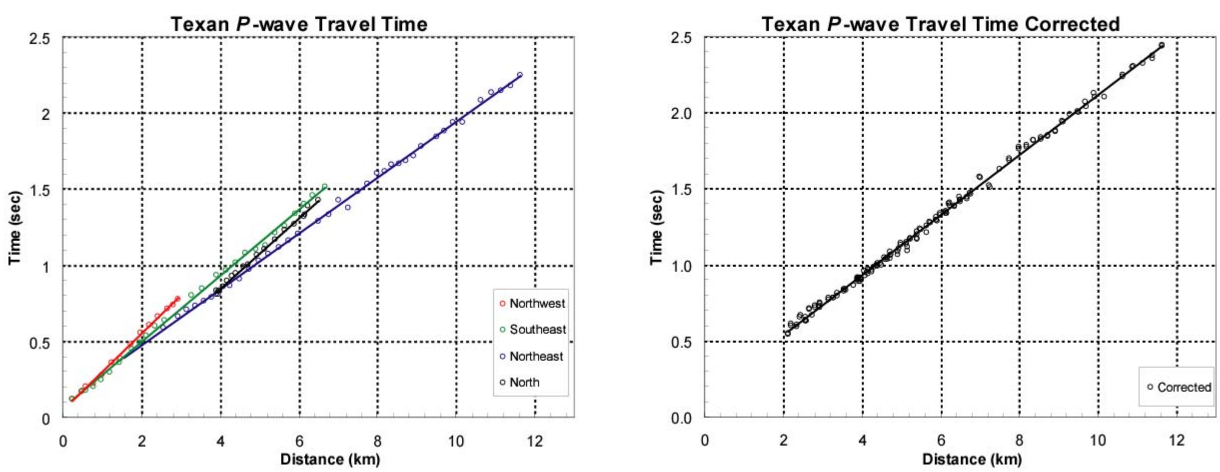

Figure 4. *P*-wave travel time plot of an FRE shot (left) recorded by the Texan network. Note the varying travel times based on station location (colored trend lines). On the right are the travel times at distances greater than 2 km for the same data after the anisotropic correction has been applied. All data can now be fit by a single velocity trend line.

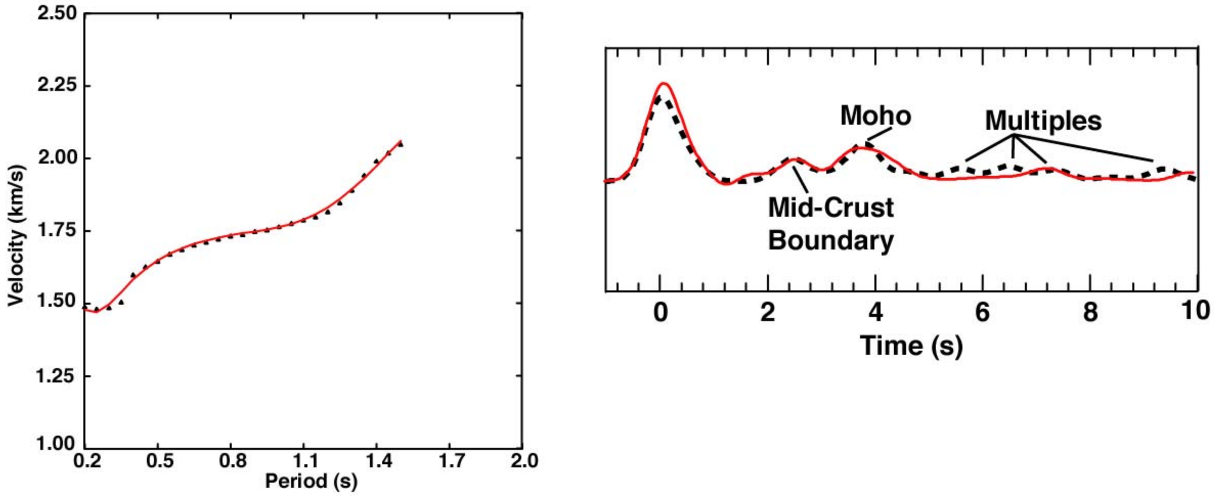

Figure 5. Plot of the best fit to a joint inversion of surface wave dispersion (left) and a receiver function (right). Black dashed lines are the observed data and red lines are the modeled data.

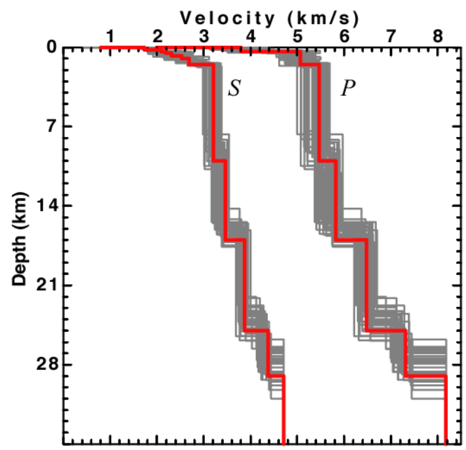

Figure 6. Best fitting 1-D velocity model (red) for the FRE test site and the range of models that satisfactorily fit the observed data (grey).

Shear Wave Generation

In theory, spherical explosion sources do not directly generate shear waves. They can indirectly generate shear energy through *P*-to-*S* reflections, *Rg* scattering, tectonic release, spall, and fracturing of the surrounding medium. Broadband transverse components show arrivals at a similar time and size as the Rayleigh wave for the FRE shots (Figure 7). This energy is interpreted to be a Love or SH wave arriving slightly prior to the Rayleigh wave. The shear energy does not seem to be affected by varying amounts of topography along the travel path, as paths completely in Goldstream Valley have large shear arrivals.

The shear arrival on Texan record sections (Figure 8) does not appear to be generated at the same time as the *P* phase. It is very difficult to pick the shear arrival at close-in stations so we cannot precisely determine the time delay or exactly where it is being generated. Examination of spall and calculations of *P*-to-*S* conversions from the free surface found that these two sources may be contributing to the shear energy, but neither were likely the primary source. Dr. Charlie Sammis has theorized that the summation of fracturing around the explosion could generate significant shear energy from an explosive source. We are providing him with data from this experiment to test this theory.

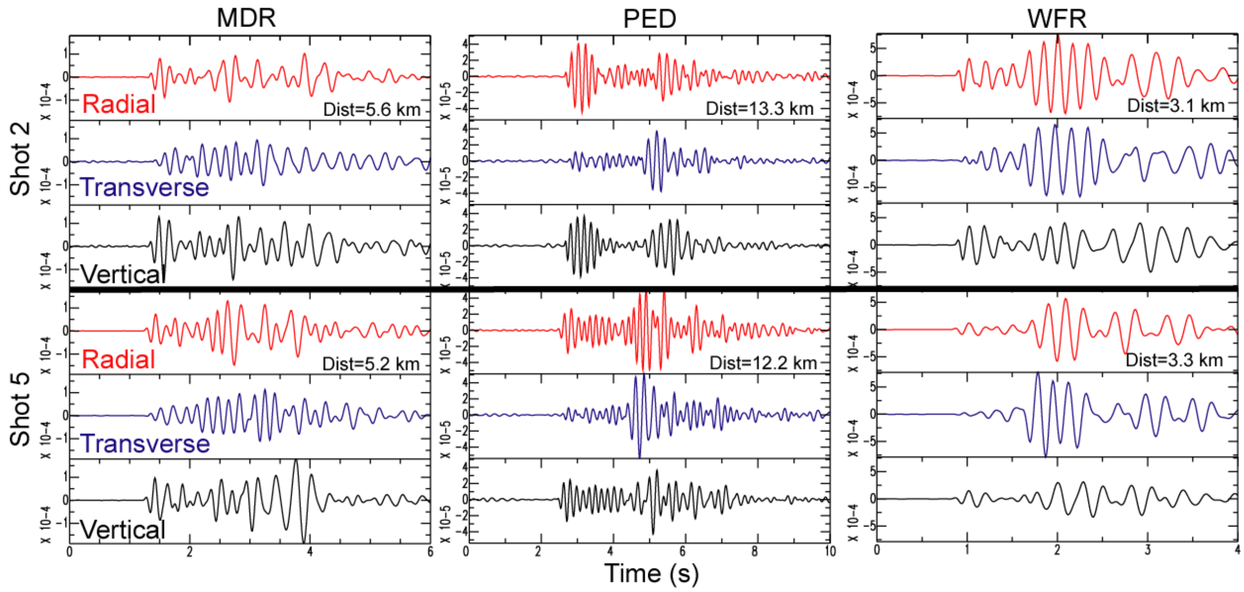

Figure 7. Three-component broadband data bandpass filtered from 3-6 Hz showing large transverse arrivals slightly earlier than the Rayleigh-wave arrival.

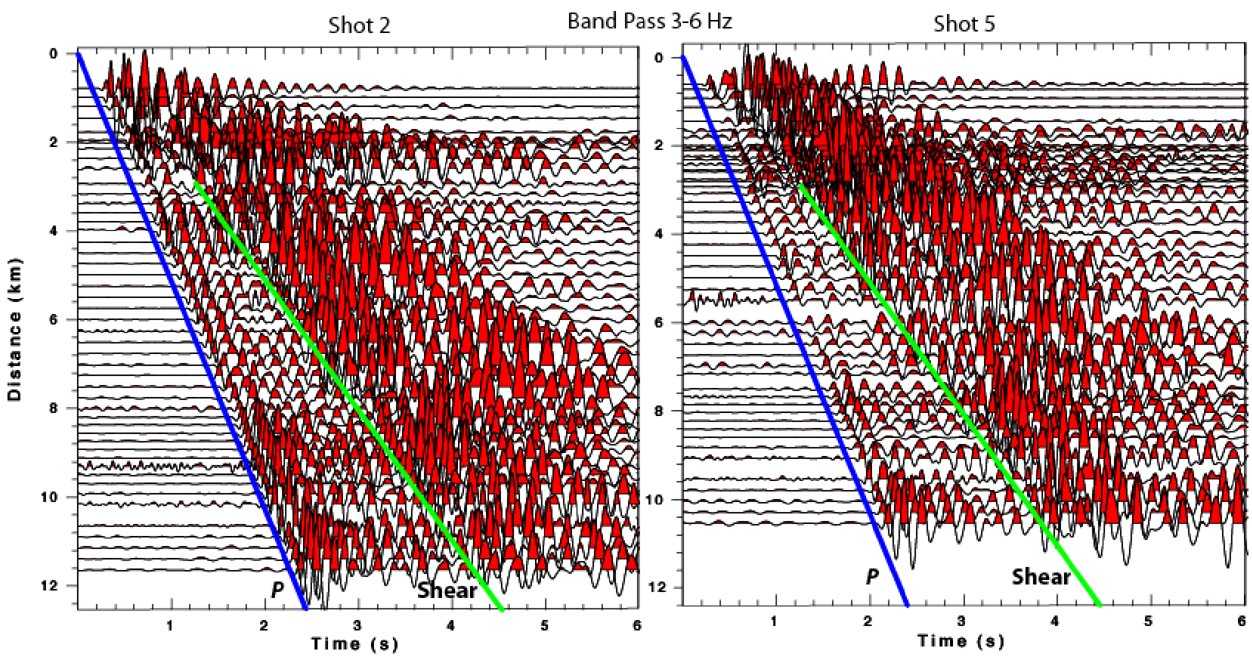

Figure 8. Texan data band passed from 3-6 Hz highlighting the *P* (blue) and shear (green) arrivals from both the frozen (shot 2) and unfrozen (shot 5) 350 lb shots.

Spectral Analysis

We calculated ratios of the full waveform FRE shot spectra to examine differences in the frozen and unfrozen explosion frequency content. In Figure 9, the Texan frozen/unfrozen spectral ratios are plotted for the 200 and 350 lb explosions. Median ratios for both size shots are very similar as are the individual ratios at each station. Below 4 Hz, the frozen shot amplitudes are ~2 times larger than the unfrozen shot amplitudes. From 4-9 Hz, the ratio drops below one suggesting that the unfrozen shots are larger in this range. The spectral ratio quickly rises to almost five above 10 Hz. This dramatic increase is likely related to the higher corner frequency for the frozen shots.

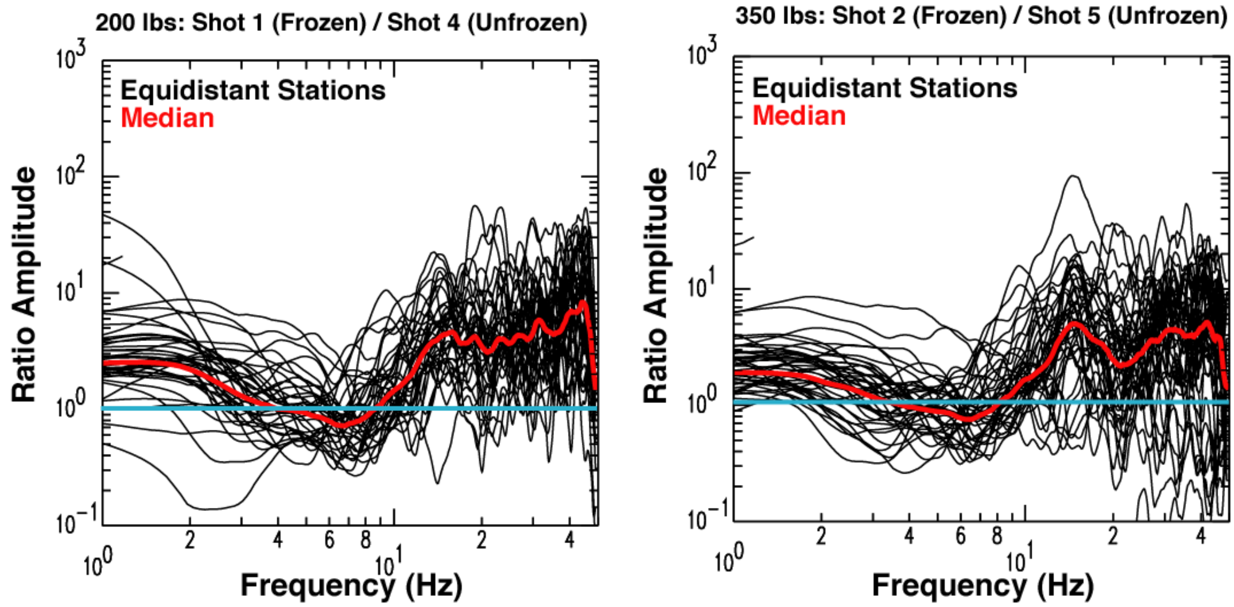

Figure 9. Spectral ratios for shot 1/shot 4 and shot 2/shot 5. Individual ratios are shown in black and the median is shown in red. A ratio greater than one indicates the frozen shot is larger than the unfrozen shot.

Mueller-Murphy Modeling

Seismic refraction studies at the two test sites suggest that the *in situ* *P*-wave velocity for the frozen rock medium was 28% faster than the unfrozen medium, while the *S*-wave velocity was 40% faster. These differences cannot be attributed only to the slight variations in the lithology between the two metamorphic assemblages and must also be related to strengthening when ice fills the cracks. When the differences in the velocities are incorporated into the Mueller-Murphy (1971) source with medium-dependent properties similar to rhyolite, we observe a good fit between observed and theoretical spectral ratios (Figure 10). The MM source with the *in situ* velocities predicts the different corner frequencies for the two media. When the laboratory-determined velocities were input into the MM source, there was considerable mismatch between the observed and theoretical ratios. The fracture networks at the two test sites, either filled with ice or air, contribute significantly to the differences in the observed seismograms.

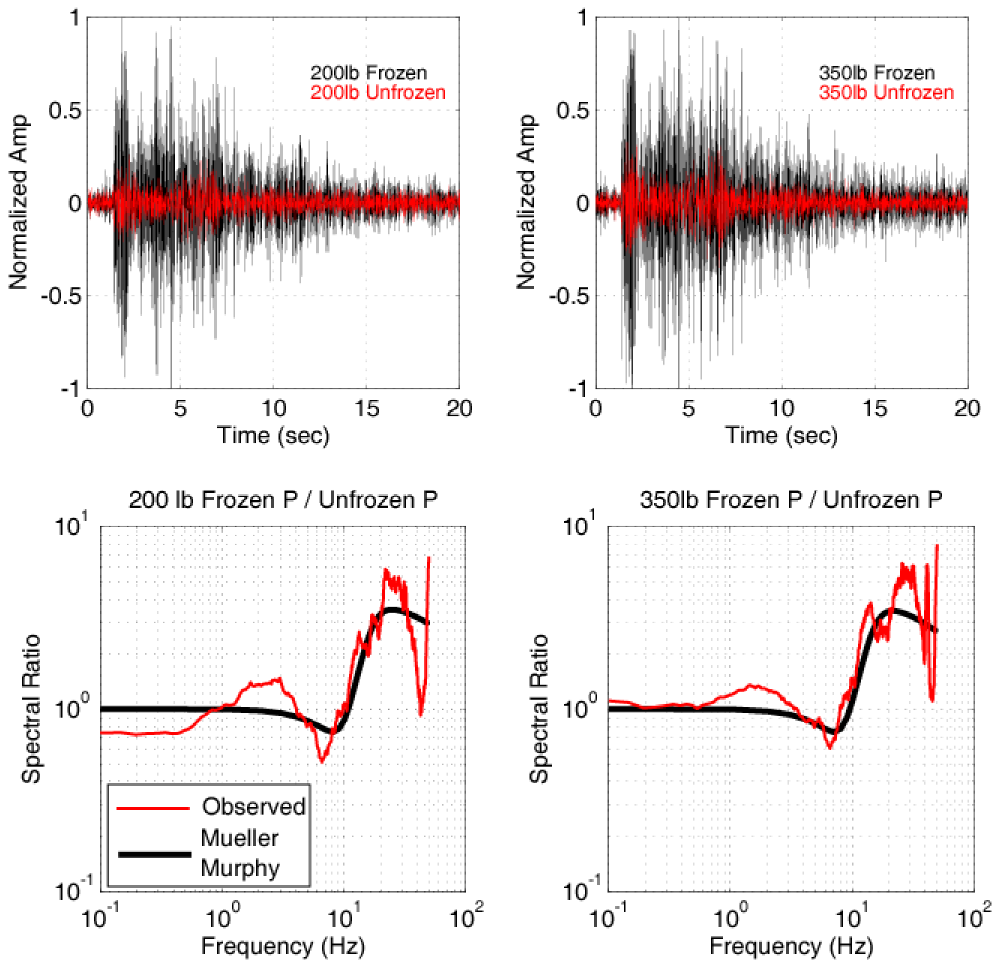

Figure 10. Amplitude differences between explosions in frozen and unfrozen rocks and the MM source. The upper plots show the waveforms recorded at 22 km from the explosions. The lower plots show the *P*-wave spectral ratios for these waveforms (red) compared to theoretical spectral ratios (black) from the MM source based on *in situ* velocity differences between the two test sites.

Phase Amplitudes

To further examine the frozen vs. unfrozen differences, the maximum amplitude of the *P*, *S*, and surface wave phases were measured on the Texan data. The Texans were deployed in a wide range of soils and gravels that caused the stations to have large amplitude variations. To avoid the site and distance effects, only stations that were equidistant to both test sites were used. In Figure 11, we plot the individual phase amplitudes and the *P*/*S* ratios for these stations.

The *P* amplitudes for shots 2 and 5 are very similar, and the same is true for shots 1 and 4, except at distances greater than 6 km where shot 1 is smaller. The unfrozen shots have significantly larger *S* amplitudes between 4 and 8 Hz. At many stations, the 200 lb unfrozen *S* amplitude is larger than the 350 lb frozen amplitude. The site effects can be observed by large scatter as a function of distance, but consistency in amplitude between shots. The unfrozen shots have larger *S* amplitudes from 2–4 Hz as well (not shown), but in the 8–16 Hz window, the frozen amplitudes are larger. Examination of the *P*/*S* ratios in Figure 11 shows larger values for the frozen shots, particularly for distances greater than 5 km. Interestingly, unfrozen shot 4 (200 lb) has larger ratios than unfrozen shot 5 (350 lb). Based on the *P* and *S* amplitude plots, it appears that this ratio difference is caused by shot 4 generating almost as much *P* energy as shot 5. A possible explanation is that shot 5 cratered while shot 4 had retarc. Surface wave amplitudes of the frozen shots are 2–3 times larger than the unfrozen shots in the 0.5–2 Hz pass band

(Figure 11). This is a surprising result and needs further study. Our future plans are to try and model the difference in the *P/S* ratios using the Mueller-Murphy source with the corner frequency scaled proportionally to the *S*-wave velocity following the methods of Fisk (2007).

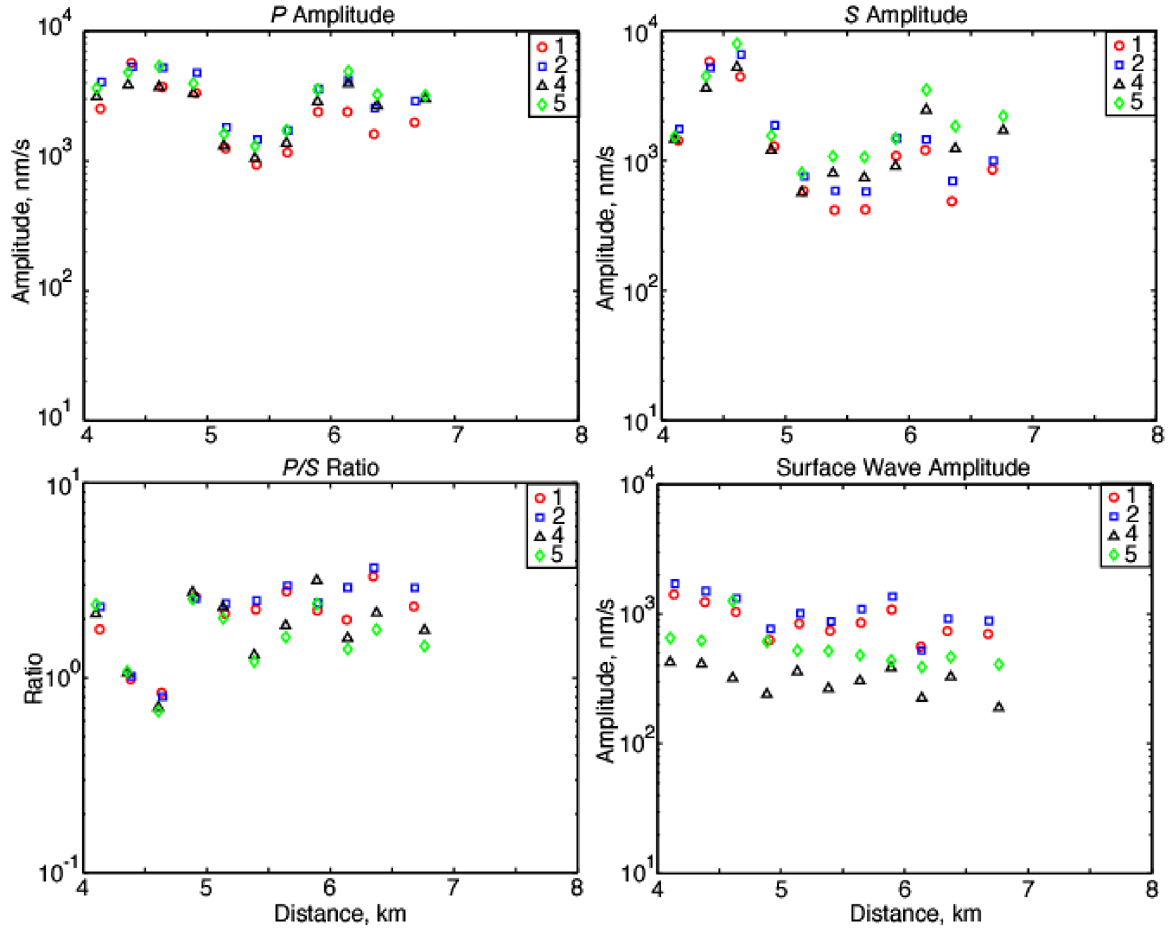

Figure 11. Phase amplitudes from equal size explosions. *P* amplitudes (upper left) are similar for the frozen and unfrozen shots. The unfrozen shots have larger *S* amplitudes though (upper right) and therefore, the *P*/*S* ratios are larger for frozen shots (bottom left). The frozen shots generated significantly more surface wave energy in the 0.5–2 Hz pass band (bottom right).

CONCLUSIONS AND RECOMMENDATIONS

The data collected from the Frozen Rock Experiment show that differences in amplitudes between our explosions at the frozen and unfrozen rock test sites are frequency dependent. The frozen rock medium was stronger and resulted in a smaller cavity radius, which increases the corner frequency when compared to the unfrozen rock medium. Above 10 Hz, the frozen explosions had significantly larger amplitudes, but between 4 and 9 Hz, the unfrozen shots produced larger amplitudes. It is expected that the amplitudes from the explosions in the unfrozen rock would have been larger had we been able to conduct them in water-saturated unfrozen rock. We are currently negotiating with landowners near the test site region to conduct another set of explosions in wet and unfrozen rock.

We have shown that the observed amplitude differences can be effectively modeled using the Mueller-Murphy (1971) source for rhyolite and the observed test site *P*- and *S*-wave velocities. The differences in the velocities for the two test site media can be attributed to two factors: a) slight lithology variations (gneiss/schist vs. schist) between the two test sites and b) strengthening caused by the ice-filled cracks in the frozen medium. Laboratory samples show 12% difference in the *P*-wave velocity between samples of the unfrozen schist and frozen gneiss/schist. In situ velocities measured from refraction studies at each test site indicate a much larger 28% difference in the *P*-wave velocities, which results in a very good fit between the observed spectral ratios and the MM source.

Larger shear wave arrivals were recorded from the shots in unfrozen schist, while larger surface waves were observed for the shots in frozen rock. There are several explanations for these phenomena that we are currently studying. First, the increased strength of the frozen rock may inhibit sliding along fractures thus reducing shear wave generation at the source. Another explanation could be that the unfrozen rock shots were detonated near the summit of a hill leading to possible *Rg-S* scattering, thus reducing the surface wave amplitudes while increasing the *S*-waves. A third explanation could be differences in the tensile strength between the frozen and unfrozen overburden, which could greatly change the properties of secondary sources such as spall and block motions.

Future research will include using ongoing moment tensor calculations to generate regional and teleseismic distance synthetic waveforms. We will then hopefully be able to determine whether explosions in frozen rock produce biased yields at the frequencies typically observed in nuclear monitoring operations. We will also continue work to document the *S*-waves generated by the FRE explosions to aid the understanding of shear wave generation from explosions.

REFERENCES

Fisk, M. (2007). Corner frequency scaling of regional seismic phases for underground nuclear explosions at the Nevada Test Site. *Bull. Seism. Soc. Am*. 97: 977–988.

Koper, K. D. M. E. Wysession, and D. A. Wiens (1999). Multimodal function optimization with a niching genetic algorithm: A seismological example, *Bull. Seism. Soc. Am*. 89: 978–988.

Mellor, M. (1971). Strength and deformability of rocks at low temperatures, Hanover, NH, Cold Regions Research and Engineering Laboratory (CRREL), U. S. Army Corps of Engineers, Research Report 294.

Mueller, R. A., and J. R. Murphy (1971). Seismic characteristics of underground nuclear detonations: Part I, Seismic scaling law of underground detonations, *Bull Seism. Soc. Am*. 61: 1675.

Sammis, C. and R. Biegel (2004). Mechanics of strengthening in crystalline rock at low temperatures: a preliminary assessment, in *Proceedings of the 26th Seismic Research Review: Trends in Nuclear Explosion Monitoring*, LA-UR-04-5801, Vol. 2, pp. 475–484.